Molecular Dynamics Simulation of a Phenylene Polymer. 3. PEEK

C. L. Chen,* C. L. Lee, H. L. Chen, and J. H. Shih

Department of Chemistry, National Sun Yat-sen University, Kaohsiung, Taiwan 804, R.O.C.

Received April 7, 1994; Revised Manuscript Received September 23, 1994®

ABSTRACT: Molecular dynamics (MD) simulation with the TRIPOS 5.2 force field was carried out on a phenylene polymer, poly(aryl ether ether ketone), in its amorphous state at two temperatures. Rotations of single phenylene rings and large segments involving five consecutive phenylene rings and four bridging atoms were investigated. The activation energies for the restricted cooperative rotations of both types of rotational units were estimated around 1.5 kcal/mol. For the restricted phenylene ring rotations, the ether–ether rings were found to be more mobile than the ether–ketone rings. On the average, the restricted rotations of large segments are less mobile than the single phenylene rings. The local environment of these large segments was found to be very similar to that in the amorphous poly(phenylene oxide).

Introduction

Poly(aryl ether ether ketone), commonly known as PEEK, is a semicrystalline polymer with a high crystalline melting point around 335 °C and a glass transition temperature around 144 °C.[1,2] These unusual properties of PEEK make it suitable for use as a high-quality engineering thermoplastic.[3] In spite of its attractive engineering properties, many efforts have been devoted to the study of the mechanistic behaviors and conformations of this particular polymer.[4–11] The reported structure of PEEK from X-ray observation shows that the carbonyl and ether angles in this polymer are all about 126°,[1,12,13] larger than the usual ether angle (ca. 110°) and carbonyl angle (ca. 120°) in aliphatic compounds. This structure was further supported by quantum mechanical MNDO calculations.[14] Starkweather and Avakian,[15] have determined the activation energy of the γ-relaxation peak of PEEK as 10 kcal/mol from dielectric measurements. This peak was assigned to the high-frequency component of a broader distribution of motions probably related to a fundamental molecular process of a noncooperative nature. Clark et al.[16] have studied the amorphous and semicrystalline samples of PEEK by using both wide-line ^{1}H NMR and cross-polarization magic-angle spinning (CP/MAS) ^{13}C NMR. In both samples, a molecular motion with an activation energy of 3.2 kcal/mol was detected. The CP/MAS spectrum of the amorphous sample displayed broader signals than did the semicrystalline sample. This suggests that it may present high-frequency molecular motions of PEEK in its amorphous state. Poliks and Schaefer[17] performed a more detailed study of molecular motions using CP/MAS ^{13}C NMR. Their result indicates that only a limited fraction of phenylene rings are mobile in amorphous PEEK. The ether–ketone rings are slightly more mobile than the ether–ether rings, but both of them are restricted. Interchain packing effects in the amorphous PEEK sample were proposed to explain the restriction of the ether–ether ring rotations. Hay and Kemmish[14] have investigated this problem by using semiempirical self-consistent field calculations on various model compounds. Their results supported the suggestion that the interchain packing effect may cause the observed inclinations of the phenylene rings along the PEEK chain as well as the variation in unit cell dimensions of PEEK with crystallization temperature.[18] Chen et al.[19] studied the segmental motions in PEEK by using CNDO/2 (complete neglect of differential overlap) calculations.[20] The result indicates that for the preferred arrangement of ether–ether rings and ether–ketone rings, medium to large amplitude rotational motions of phenylene rings are energetically possible in the amorphous state. All the experimental and theoretical results indicate that various types of molecular motion may exist in amorphous PEEK and that interchain packing may have a significant effect on the segmental motions.

Reported here are our recent results on the segmental motions of PEEK in the amorphous state by molecular dynamics (MD) simulation. This is a continuation of our earlier work on the MD simulation of poly(phenylene oxide) (PPO). The results for amorphous PEEK are compared to the results for PPO.[21]

Systems and Simulation

Given in Figure 1 is the repeating unit of PEEK. Our model chain of PEEK consists of 20 repeating units with two phenylene rings at both ends of the chain. The construction of the amorphous PEEK system is the same as described in our previous investigation of PPO.[21] Periodic boundary conditions and the mirror image convention were used. The box size was adjusted until the density of the system matched the desired value of 1.265 g/cm^3.[1,2] The systems were prepared at two different temperatures, ambient temperature (300 K) and high temperature (410 K), which are below the glass transition temperature. The former is referred to as the ambient temperature system (ATS), and the latter is referred to as the high-temperature system (HTS).

The MD simulation was carried out with the use of the modified TRIPOS 5.2 force field.[22] The force field can be expressed as

$$V = V_{vdw} + V_s + V_b + V_t + V_{pl}$$

where V_{vdw} is the long-range van der Waals interaction term, V_s is the bond stretch potential, V_b is the angle bending potential, V_t is the torsional potential, and V_{pl} is the out-of-plane bending potential. In the TRIPOS

* To whom correspondence should be addressed.

® Abstract published in *Advance ACS Abstracts,* November 15, 1994.

0024-9297/94/2227-7872$04.50/0

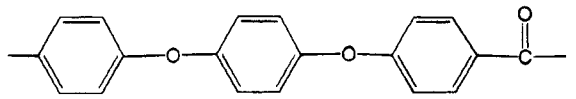

Figure 1. Structure of the repeating unit of PEEK.

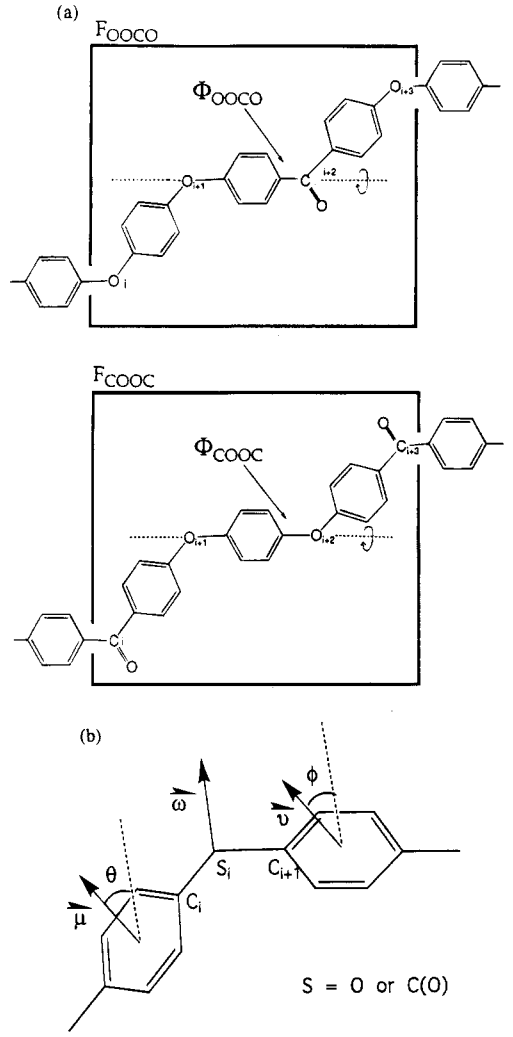

Figure 2. Definitions for (a) torsional angles Φ_{OOCO} and Φ_{COOC} and (b) paired dihedral angles $(\theta,\phi)_s$, s = O or C(O). Vector ω is normal to the $C_i-S_i-C_{i+1}$ plane, vector μ is normal to the plane of the ith phenylene ring, and vector ν is normal to the plane of the $(i+1)$th phenylene ring. θ and ϕ are the dihedral angles between μ and ω and between ν and ω, respectively.

force field, V_b has the form $V_b = K_b(\theta - \theta_0)^2$, where θ_0 is 120° for the carbonyl and 110° for the ether. In our simulation, the value of θ_0 is selected as 126° for both the carbonyl and ether angles. This selection is based on crystallographic information[1,12,13] and the results of semiempirical molecular orbital calculations.[14] The Beeman algorithm[23] was used in the simulation. The cutoff distance was chosen at 10 Å, and a relatively small time step, 0.2 fs, was used due to the fast vibration of the CH bond. Both systems were pre-equilibrated, and trajectories were collected and analyzed over 60 ps after equilibrium.

Results and Discussion

Two types of segmental motion in amorphous PEEK were investigated: the restricted rotation of the phenylene rings and the torsion of a large segment consisting of five consecutive phenylene rings and four bridging atoms. Figure 2a illustrates these large segments: F_{OOCO} (fragment constituted by −O−O−C(O)−O−) and

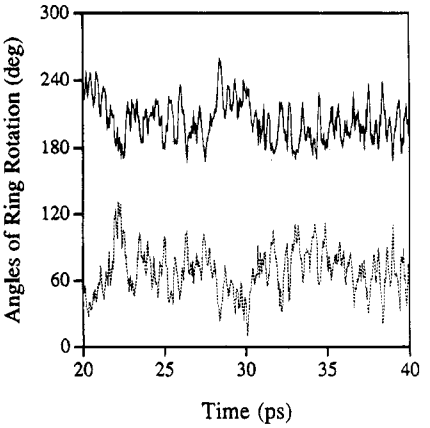

Figure 3. Trajectories of the 5th paired dihedral angles, θ (solid line) and ϕ (dashed line) at ATS.

F_{COOC} (fragment constituted by −C(O)−O−O−C(O)−). The torsional angles of F_{OOCO} and F_{COOC} are denoted Φ_{OOCO} and Φ_{COOC}. The definitions of the dihedral angles are given in Figure 2b. The dihedral angles of paired adjacent phenylene rings are referred to as $(\theta,\phi)_s$, where the subscript s represents the linking atom (O = ether oxygen atom and C(O) = carbonyl carbon atom) between the phenylene rings.

1. Cooperativity of Phenylene Ring Rotation. Given in Figure 3 are the trajectories of $(\theta_5,\phi_5)_O$ at ATS. The subscripts of θ and ϕ indicate the numbers of dihedral angles counted from one end of the chain. The figure shows that these two angles are changed simultaneously. This indicates that adjacent phenylene rings rotate cooperatively in an in-phase manner. Throughout the simulation, we found that all the cooperative ring rotations are in-phase rotations. For ATS, we found that 17 pairs of phenylene rings have moderate-amplitude (ca. 60°) cooperative rotations and 2 pairs of phenylene rings have large-amplitude (ca. 120°) cooperative rotations. For HTS, we found that 28 pairs of phenylene rings have moderate-amplitude cooperative rotations and 10 pairs of phenylene rings have large-amplitude cooperative rotations. Therefore, the simulation indicates that the occurrence of the cooperative rotations of the phenylene rings and the amplitudes of these rotations are sensitive to temperature. The numbers of cooperative phenylene ring rotations with amplitudes larger than 60° are 19 at 300 K and 38 at 410 K. We assume that this type of rotation follows the Arrhenius equation,

$$f \propto k = A \exp(-\Delta E/k_B T)$$

where f is the frequency, k is the rate constant, A is the pre-exponential factor, ΔE is the average energy barrier, k_B is the Boltzmann constant, and T is the absolute temperature. Substituting the observed values and temperatures into this equation, ΔE is estimated as 1.5 kcal/mol. This value can be checked by comparing the calculated potential energy maps of diphenyl ether (DPE) and diphenyl ketone (DPK). The energy map of DPE calculated with the use of the TRIPOS 5.2 force field has been reported in our previous work on PPO.[21] Given in Figure 4 is a similar energy map for DPK. This map was calculated at a fixed carbonyl angle (126°), fixed bond lengths, and fixed bending angles but the dihedral angles of the phenylene rings were allowed to vary. Both maps show that the low-energy regions for the synchronously restricted rotations of the phenylene rings are lower than 2 kcal/mol. This supports the

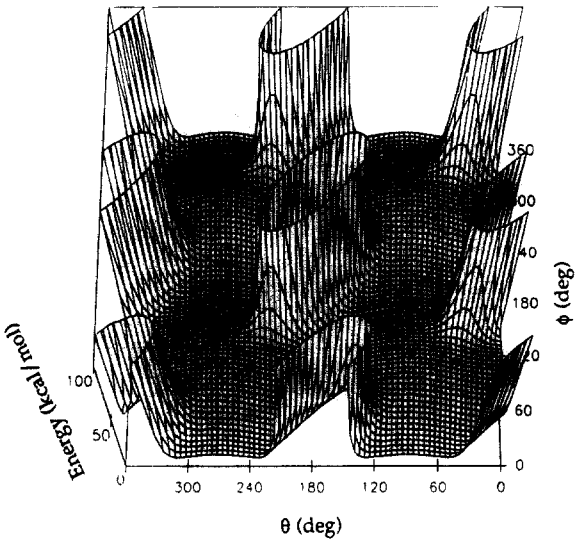

Figure 4. Conformational potential energy surface of DPK evaluated with the TRIPOS 5.2 force field.

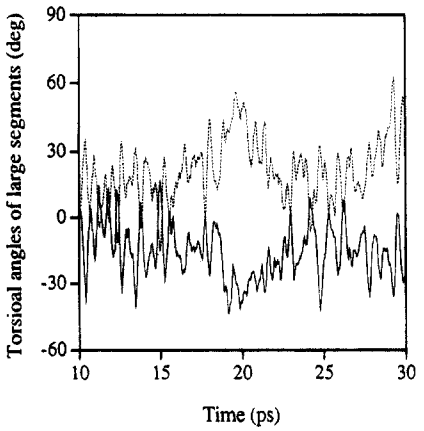

Figure 5. Φ trajectories of the 15th torsional angle (solid line) and the 16th torsional angle (dashed line) of large segments at HTS.

estimated value of the energy barrier from the MD simulation.

2. Cooperativity of Large-Segment Torsion. Given in Figure 5 are the trajectories of the 15th and 16th torsional angles of the large segments for HTS. These two angles are Φ_{COOC} and Φ_{OOCO}, respectively. The figure shows that these two angles are changed simultaneously in opposite directions. Therefore, it is an out-of-phase cooperative torsion. As discussed earlier in the work on PPO,[21] the out-of-phase cooperative rotation for a large segment is preferred since less free volume is required. For ATS, we found 10 moderate-amplitude cooperative torsions and 1 large-amplitude cooperative torsion. For HTS, we found 15 moderate-amplitude cooperative torsions and 6 large-amplitude cooperative torsions. Therefore the occurrence of cooperative torsions and their amplitudes are also sensitive to temperature. The numbers of occurrence and the temperature dependence indicate that this large-segment torsion has a comparable energy barrier to the cooperative rotation of the phenylene ring. This implies that the PEEK chain is quite flexible at least within the length of 2 repeating units.

3. Restricted Rotation of Phenylene Ring. The rotational diffusion coefficient (RDC), D, of a phenylene ring can be calculated by the mean square displacement of the rotation angle, θ,

$$2Dt = \lim_{t\to\infty} \langle|\theta(t) - \theta(0)|^2\rangle$$

where the angular brackets denote the long-time average. Given in Table 1 is a summary of the calculated RDCs of ether–ether ring and ether–ketone ring at two different temperatures. The RDC of the phenylene ring of PPO at 300 K is also listed in the table for comparison. The result shows that the RDCs of ether–ether rings are larger than the RDCs of ether–ketone rings at both temperatures. These coefficients are greater at the higher temperature than at the lower temperature. At 300 K, the RDC of the ether–ether ring is larger than the RDC of the phenylene ring in the PPO system while the RDC of the ether–ketone ring is smaller. The average value of the RDC of the ether–ether ring and the RDC of the ether–ketone ring is 4.69 deg²/ps. (Note that our chain consists of 20 ether–ether rings and 39 ether–ketone rings.) This value is smaller than that of PPO.[21] The magnitude of the RDC is an indication of the mobility of the rotation of phenylene ring rotation in the polymer. Our simulation shows that the ether–ether rings in PEEK are more mobile than the phenylene rings in PPO for ATS. On the other hand, the ether–ketone rings in PEEK are less mobile than the rings in PPO. On the average, the mobility of the phenylene ring in amorphous PEEK is less than that of the rings in amorphous PPO. Given in Figures 6 and 7 are the simulated populations of rotational angles of the ether–ether ring and the ether–ketone ring around their average values at two temperatures. At both temperatures, the population of ether–ether rings is broader than the population of ether–ketone rings. At higher temperature, the populations of both rings are broader than at low temperature. This indicates that the amplitude of the rotation of the ether–ether ring is larger than that of the ether–ketone ring in amorphous PEEK. In comparison with the similar distribution of phenylene rings in amorphous PPO, we found that both ether–ether rings and ether–ketone rings are more restricted than rings in PPO at 300 K.[21] This restriction is attributed to the different interchain interactions in amorphous PEEK and PPO.

4. Restricted Torsion of Large Segment. The estimated RDCs for F_{OOCO} and F_{COOC} with respect to the torsional angles, Φ_{OOCO} and Φ_{COOC}, are summarized in Table 1. The RDC for the corresponding four-oxygen segment (FOS) of PPO is also listed for comparison. At 300 K, the RDC of F_{COOC} is slightly larger than the RDC of F_{OOCO}. On the other hand, at 410 K the RDC of F_{OOCO} is larger than the RDC of F_{COOC}. This implies that at 300 K the hindrance that come from the local environment of F_{COOC} and F_{OOCO} are of the same magnitude, but at 410 K the hindrance to F_{COOC} is larger than that to F_{OOCO}. At both temperatures, the RDCs for these segments are larger than the RDC of the ether–ketone ring but smaller than the RDC of the ether–ether ring or smaller than the average RDC of the phenylene rings. This indicates that F_{OOCO} and F_{COOC} are less mobile than the rings in amorphous PEEK. Given in Figures 8 and 9 are the simulated populations of Φ_{OOCO} and Φ_{COOC} around their average values. The simulation shows that the average amplitudes of these restricted torsions are around 45° at 300 K and around 60° at 410 K. The RDCs for the large segments of F_{OOCO} and F_{COOC} in PEEK are somewhat larger than the RDC of FOS in PPO. However, these RDCs are all of the same order of magnitude. The amplitudes of F_{OOCO} and F_{COOC} in PEEK are ±45°, which is about the same as the

Table 1. RDCs (deg^2/ps) of PEEK and PPO at 300 and 410 K

type	300 K	410 K
PEEK		
ether–ether ring	8.12	15.31
ether–ketone ring	2.93	6.52
F_{OOCO}	4.11	12.35
F_{COOC}	4.56	8.84
PPO[a]		
phenylene ring	5.67	
FOS	3.18	

[a] RDCs of PPO were adopted from ref 21.

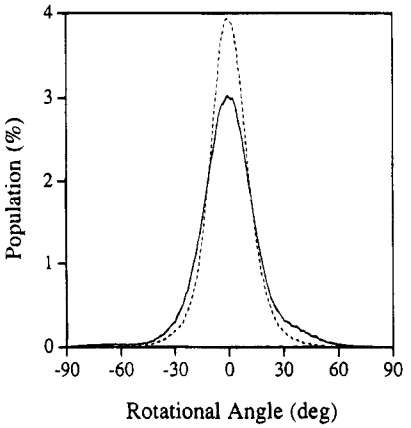

Figure 6. Population of rotational angles of the ether–ether ring (solid line) and the ether–ketone ring (dashed line) around their average values at ATS.

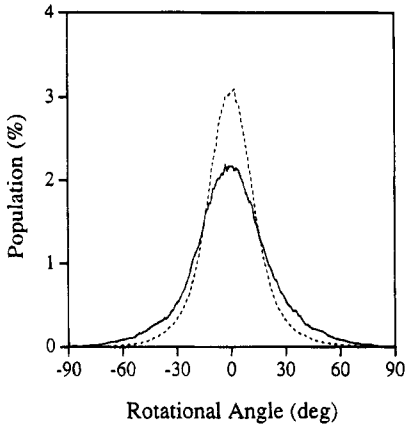

Figure 7. Population of rotational angles of the ether–ether ring (solid line) and the ether–ketone ring (dashed line) around their average values at HTS.

amplitude of FOS in PPO. Therefore, in these polymers, the hindrance that comes from the local environment of these large segments should be very similar.

Conclusions

By means of MD simulation, we have analyzed the cooperative rotations of phenylene rings and large segments, F_{OOCO} and F_{COOC}. The activation energy barriers for these cooperative rotations were estimated around 1.5 kcal/mol. The restricted rotations of the phenylene rings and the large segments were also analyzed. Our result shows that the ether–ether rings are more mobile than the ether–ketone rings. On the average, the mobility of the phenylene rings in amorphous PEEK is less than the mobility in amorphous PPO. In the analysis of the restricted rotations of the large segments, we found that the mobility of the large segments is less than the average mobility of the

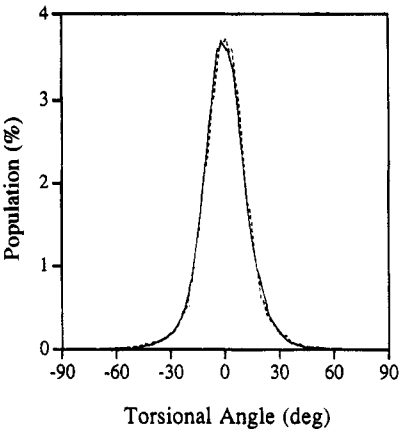

Figure 8. Population of torsional angles F_{OOCO} (solid line) and F_{COOC} (dashed line) around their average values at ATS.

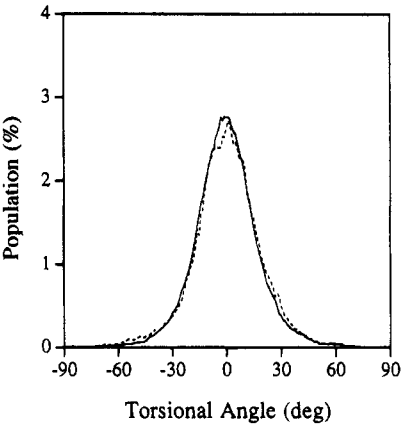

Figure 9. Population of torsional angles, F_{OOCO} (solid line) and F_{COOC} (dashed line) around their average values at HTS.

phenylene rings. We also found that the local environment of these large segments in amorphous PEEK is similar to that in amorphous PPO. The glass transition temperature of PEEK is much higher than the glass transition temperature of PPO. Therefore, our simulation implies that the difference in T_g between these two polymers should involve interactions or cooperativity beyond the segments comprising four or five phenylene rings.

Acknowledgment. This work was carried out on a CONVEX C3840 computer at NSYSU. Thanks are due to the computer center at NSYSU for their help. Valuable suggestions from and discussions with Prof. A. C. Su of the Institute of Material Science and Engineering are gratefully acknowledged. We wish to thank a referee of this paper for many valuable suggestions. This work is financially supported by the National Science Council, Republic of China, under Contract No. NSC-83-0208-M-110-023.

References and Notes

(1) Dawson, P. C.; Blundell D. J. *Polymer* **1980**, *21*, 577.
(2) Sasuga, T.; Hagiwara, M. *Polymer* **1985**, *26*, 501.
(3) Cattanach, J. B.; Cogswell, F. N. In *Developments in Reinforced Plastics—5*; Pritchard, G., Ed.; Applied Science (Elsevier): New York, 1986; Chapter 1.
(4) Blundell, D. J.; Osborn, B. N. *Polymer* **1983**, *24*, 953.
(5) Lazzaroni, R.; Sato, N.; Salaneck, W. R.; Dos Santos, M. C.; Bredas J. L.; Tooze, B.; Clark, D. T. *Chem. Phys. Lett.* **1990**, *175*, 175.
(6) Michele, A.; Vittoria, V. *Polym. Commun.* **1991**, *32*, 232.
(7) Grayson, M. A.; Wolf, C. J. *J. Appl. Polym. Sci.* **1991**, *42*, 543.
(8) Mehmet-Alkan, A. A.; Hay, J. N. *Polymer* **1992**, *33*, 3527.

(9) Zhang, Z. Y.; Zeng, H. J. *J. Appl. Polym. Sci.* **1993**, *48*, 1987.
(10) Jonas, A.; Legras, R.; Scherrenberg, R.; Reynasers, H. *Macromolecules* **1993**, *26*, 526.
(11) Jonas, A.; Legras, R. *Macromolecules* **1993**, *26*, 813.
(12) Rueda, D. R.; Ania, F.; Richardson, A.; Ward, I. M.; Calleja, F. J. B. *Polymn. Commun.* **1983**, *24*, 258.
(13) Hay, J. N.; Kemmish, D. J.; Langford, J. I.; Rae, A. I. M. *Polym. Commun.* **1984**, *25*, 175.
(14) Hay, J. N.; Kemmish, D. J. *Polym.* Commun. **1989**, *30*, 77.
(15) Starkweather, H. W., Jr.; Avakian, P. *Macromolecules* **1989**, *22*, 4060.
(16) Clark, J. N.; Jagannathan, N. R.; Herring, F. G. *Polymer* **1988**, *29*, 341.
(17) Poliks, M. D.; Schaefer, J. *Macromolecules* **1990**, *23*, 3426.
(18) Hay, J. N.; Langford, J. I.; Lloyd, J. R. *Polymer* **1989**, *30*, 489.
(19) Chen, C. L.; Chang, J. L.; Su, A. C. *Macromolecules* **1992**, *25*, 1941.
(20) Pople, J. A.; Beveridge, D. L. *Approximate Molecular Orbital Theory*; McGraw-Hill: New York, 1970.
(21) Chen, C. L.; Chen, H. L.; Lee, C. L.; Shih, J. H. *Macromolecules* **1994**, *27*, 2087.
(22) Clark, M.; Cramer, R. D., III; Van Opdenbosch, N. *J. Comput. Chem.* **1989**, *10*, 982.
(23) Beeman, D. *J. Comput. Phys.* **1976**, *20*, 130.